Total Ionization Dose Effects on Charge Storage Capability of Al₂O₃/HfO₂/Al₂O₃-Based Charge Trapping Memory Cell *

Yan-Nan Xu(徐彦楠)[1,2], Jin-Shun Bi(毕津顺)[1**], Gao-Bo Xu(许高博)[1], Bo Li(李博)[1], Kai Xi(习凯)[1],
Ming Liu(刘明)[1], Hai-Bin Wang(王海滨)[3], Li Luo(骆丽)[4]

[1]*Institute of Microelectronics, Chinese Academy of Sciences, Beijing 100029*
[2]*University of Chinese Academy of Sciences, Beijing 100049*
[3]*School of Internet of Things Engineering, HoHai University, Changzhou 213022*
[4]*Beijing Jiaotong University, Beijing 100044*

Because of the discrete charge storage mechanism, charge trapping memory (CTM) technique is a good candidate for aerospace and military missions. The total ionization dose (TID) effects on CTM cells with Al₂O₃/HfO₂/Al₂O₃ (AHA) high-k gate stack structure under in-situ 10 keV x-rays are studied. The C–V characteristics at different radiation doses demonstrate that charge stored in the device continues to be leaked away during the irradiation, thereby inducing the shift of flatband voltage (V_{fb}). The dc memory window shows insignificant changes, suggesting the existence of good P/E ability. Furthermore, the physical mechanisms of TID induced radiation damages in AHA-based CTM are analyzed.

As flash memory technology is advancing, the dimensions of memory cells continues to be shrunk to achieve a balance between low cost and high performance. As a result, the integration density and the memory capacity will increase simultaneously. However, there is tremendous challenge for the traditional non-volatile floating gate (FG) flash memory below 20 nm technology node, for instance, parasitic coupling effects as well as increasing leakage current. Not surprisingly, the data retention performance of these devices is getting worse.[1−5] If there is a leakage path, the CTM technique is capable of suppressing the FG coupling and retaining most of the charges because of its discrete charge storage.[6] The CTM technique with oxide-nitride-oxide (ONO) and high-k dielectric stack structure is therefore applied to the commercial complementary-metal-oxide-semiconductor (CMOS) process; and thus this technique is a promising candidate for FG flash memory.[7]

The electronic devices for space exploration missions need to operate under the harsh radiation environment. A variety of charged particles and rays, i.e., electrons, protons and heavy ions, alter the electrical performance of integrated circuits.[8] The major concerns are total ionization dose effects (TID) and single event effects (SEE). The TID effects on the non-volatile memory (NVM) may cause the loss of storage charge; and this will increase the leakage current and may even lead to functional failure. Non-volatile memory in the aerospace electronic system usually stores critical programs or data so that such errors may lead to disastrous system failures. Accordingly, it is necessary to investigate and characterize radiation effects in novel non-volatile memory devices.

The community has studied ONO-based CTM structures[9−11] and previous results show that this structure has better radiation tolerance than the traditional FG technique. High-k dielectrics can be used in CTM for the nanoscale CMOS technique[12] and there are some reports on w.r.t. radiation effects on logical devices with high-k gate oxide.[13,14] However, to our best knowledge, there are very few reports on high-k based. In this work, the TID effects on CTM cells with Al₂O₃-HfO₂-Al₂O₃ structure under 10 keV x-rays are studied. Particularly the electrical degradations with physical insights are primarily studied.

Silicon (100) substrates with p-type doping concentration of $(1–2)×10^{15}$ cm⁻³ are employed to fabricate the high-k metal gate MOS capacitors (MOSCAPs). After the standard cleaning process, a silicon wafer is treated with buffered oxide etchant (BOE) to remove nature oxide. SiO_x is grown on the wafer surface through O_3 chemical oxidation. Next, Al₂O₃(5 nm), HfO₂(6 nm) and Al₂O₃(10 nm) layers are deposited onto the SiO_x buffer layer by atomic layer deposition (abbreviated as ALD) and treated through post deposition annealing (abbreviated as PDA) under rapid thermal annealing (abbreviated as RTA) at 450℃ in N₂ ambient. Then, TiN/W metal gate is deposited on the high-k dielectric by ALD and patterned by dry etch using BCl₃+SF₆ mixed gas. The area of the capacitor is $1 × 10^{-4}$ cm². Finally, all the samples are metallized with Al (Si) on backside at 380℃ in N₂ ambient for 40 min. The illustrated structure and the cross-sectional transmission electron microscope (TEM) of the CTM MOS capac-
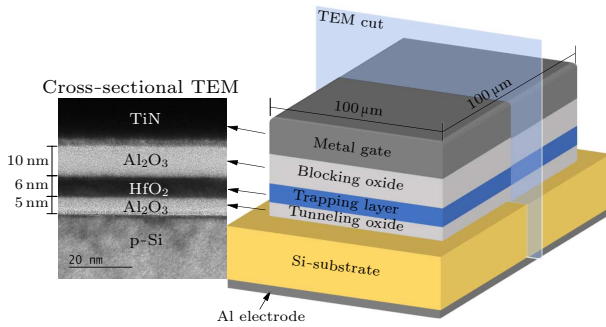
---

itor are shown in Fig. 1.

Fig. 1. The illustrated structure and cross-sectional TEM of AHA MOS capacitor.

The samples (bare dies) undergo radiation of 10 keV x-rays at a dose rate of 100 rad(Si)/s with electrically floating or the 1 V bias on the gate electrode (backside grounded). The 1 V bias state is to exert an electric field (0.5 MV/cm) without affecting the state of the memory device and the electrically floating state is for comparison. The highest total dose in this work is 290 krad(Si). Before and after the irradiation, 1 MHz C–V characteristics are measured and recorded using an Agilent B1500. The value of V_{fb} is extracted by fitting the measured C–V data to C–V simulation results using a program from UC Berkeley including the quantum mechanical effect. The experiment is performed at the x-ray on-line radiation platform (similar to Aracor 4100[15,16]) of Xinjiang Technical Institute of Physics & Chemistry, Chinese Academy of Sciences.

There are three operating states for the CTM capacitor, i.e., initial, programmed, and erased states. The initial state is the as-grown state of the device without charge storage. The device is in the programmed state when a specific positive pulse is introduced to the gate and electrons can cross the tunneling oxide and be trapped. Conversely, stored electrons can be removed when a specific negative pulse is applied to the gate. The initial-state device should be first programmed. After that, it is able to switch between programmed and erased states.

The C–V curves of an initial-state capacitor with different radiation doses are shown in Fig. 2(a). The capacitor is electrically floating during irradiation. As the dose increases, the curves shift toward the negative direction and this suggests net positive radiation-induced charges. Flatband voltage (V_{fb}) shift with respect to radiation dose is shown in Fig. 2(b). It decreases rapidly to 70 krad(Si) and then slowly gets saturated at approximately 0.65 V. The trend fits very well by an exponential function. This is explained as follows: the device at initial state has many empty traps and the radiation-induced charges can gradually fill them. As the number of empty traps decreases, the

filling process tends to get slower and eventually saturate.

The V_{fb} shift of programmed devices under x-ray radiation is shown in Fig. 3. Different flatband voltages before radiation are consistent with various amounts of electron charge storage. Comparing the results of samples 1 and 3 (or 2 and 4), it is suggested that the final V_{fb}'s will be almost the same regardless of the initial V_{fb} if the biases are the same. The results of samples 1 and 2 (or 3 and 4) suggest that positive gate bias can degrade V_{fb} more severely than the electrically floating case.
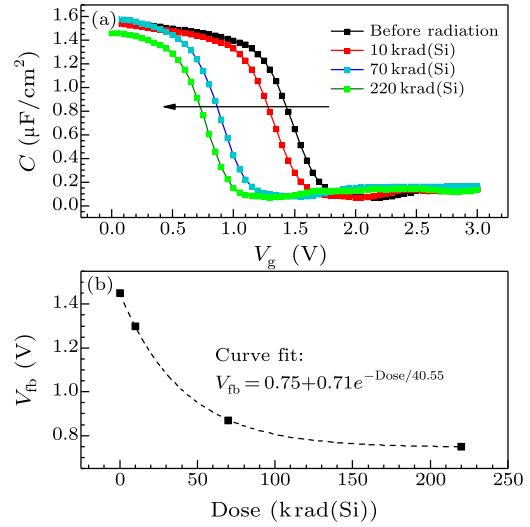

Fig. 2. (a) The 1 MHz C–V characteristics of the AHA MOS capacitor and (b) flatband voltage shift of the AHA MOS capacitor with respect to TID irradiation.
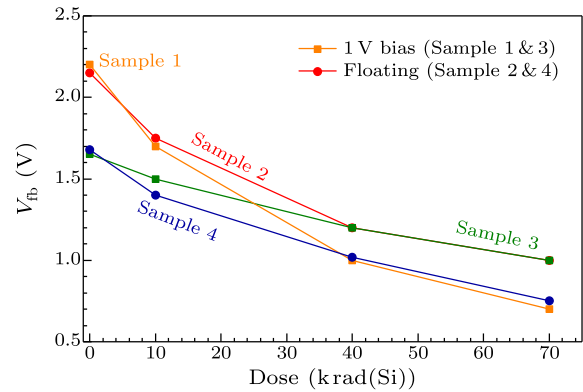

Fig. 3. The V_{fb} shift under x-ray radiation with different initial states and bias conditions.

Scanning the device C–V characteristics bi-directionally with different voltage ranges, the charges can be injected into (programmed) or discharged (erased) from the traps by crossing the tunneling layer (Al_2O_3) with the Fowler–Nordheim (FN) tunneling mechanism, causing a hysteresis window. The V_{fb} difference between the programmed and erased states is defined as the dc memory window. The 1 MHz C–V dc characteristics of the sample are shown in Fig. 4(a), and the V_g sweep direction is shown in the inset figure. There is almost no memory window for [−5 V, 5 V]

range sweep, while the memory windows are nearly 1.8 V for [−7 V, 7V] range sweep and 4.9 V for [−11 V, 11 V] range sweep.
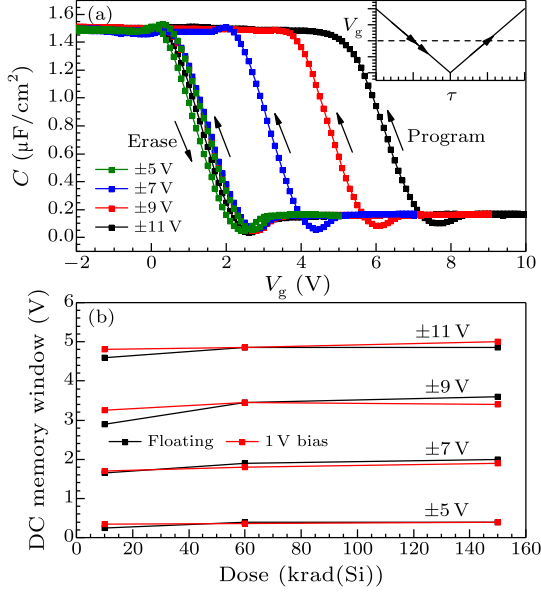

Fig. 4. (a) The dc sweep of the fresh AHA MOS capacitor. (b) The dc memory windows are almost unaffected by the total dose of x-rays.

The dc memory window of the sample affected by x-ray irradiation is shown in Fig. 4(b). It is suggested that the window is not affected at all. As noted above, we know that dc memory window reflects the ability of capturing (program) and discharging (erase) the charge. The dc sweep induced charge/discharge effects rely on the number of traps in the gate stack. The traps are primarily comprised of two parts, i.e., x-ray-induced defects in high-k dielectric (both HfO_2 and Al_2O_3) and intrinsic trapping sites for charge storage. Thus the results in Fig. 4(b) indicate that the intrinsic trapping sites in the AHA structure are much stable and the high-k materials like HfO_2 and Al_2O_3 have pretty good radiation resistance.
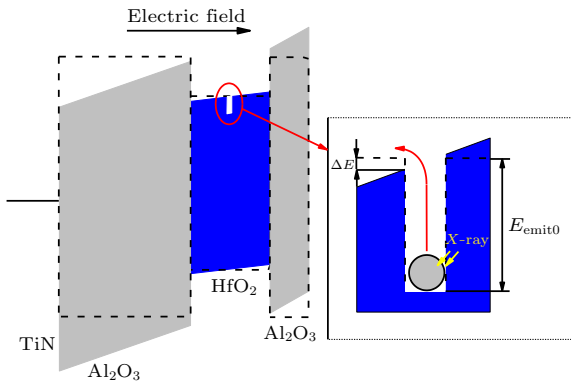

Fig. 5. Trapped electrons emission under x-ray irradiation. Here E_{emit0} denotes the activation energy for emission from the trap when $V_g = 0$ V, and ΔE is the energy difference between E_{emit} at $V_g = 0$ V and $V_g = 1$ V)

The V_{fb} reduction is clarified as two physical mech-

anisms. The first one refers to the emission of storage electrons from the traps, as shown in Fig. 5. Storage electrons absorbing energy from x-rays may be emitted from the traps and transport along electric field direction. The emission probability relies on the traps properties (including energy level depth, distribution, etc.), and the absorbed energy from radiation sources. The emission rate is defined as[17]

$$e_{FP} = v \cdot \exp\left[-\frac{q(E_{emit} - \sqrt{qE_{sin}/\pi\varepsilon_{sin}})}{kT} \right], \quad (1)$$

where v denotes the escape factor, q is the electron charge, E_{emit} is the trap energy depth, E_{sin} is the electric field across the trapping layer, ε_{sin} is the permittivity of HfO_2, k is the Boltzmann constant, and T is the absolute temperature.

The reduction of V_{fb} will be larger when the external positive voltage is applied during irradiation. This is because E_{emit} is reduced to $E_{emit0} - \Delta E$ (shown in Fig. 5(b)), and the emission becomes easier so that more electrons will be emitted from traps. As the quantity of charge continues to decrease, the internal electric field becomes progressively weaker. In the meantime, emission probability decreases. All these factors translate to the nonlinear degradation trend in Fig. 3.

The second mechanism refers to the charge generation and trapping in the high-k oxide. The ionizing radiation yields electron-hole (e-h) pairs in the bulk oxide. The quantity of generation charge is proportional to the thickness of the oxide.[18] A fraction of e-h pairs can escape from the initial recombination and yield free electrons/holes. The residual holes drift toward to the Si substrate, while residual electrons drift toward to TiN metal gate. Some of them can successfully escape from the gate without affecting the device, but the rest will be captured by traps. The radiation-induced-traps in oxide (type I)[13,19] and at Al_2O_3/Si interface (type II),[19] the intrinsic traps inside the HfO_2 (type III) and at the HfO_2/Al_2O_3 interface caused by inter-diffusion (type IV).[20] Type I is formed by the radiation-generated holes remaining in the oxide due to their relatively small mobility, which increases the net positive charges. Type II is electron trap due to O_2^- coupled to Al ion and increasing the net negative charges, whereas the trapped charges in these two processes are in the range of 10^{10}–10^{11} cm^{-2},[19] and the V_{fb} shift caused by this (<0.2 V after 100 krad(Si) irradiation) can be neglected. The charges can also be trapped in types III and IV, but the emission process we mentioned above can happen again. Thus there will be a trade-off between the emission process and the capture process. Wide bandgap high-k materials can make it more difficult to yield radiation-induced e-h pairs. Furthermore, the traps with deeper energy levels have better charge retention so that the anti-TID effects capacity can be significantly improved.

In conclusion, the TID effects of 10 keV x-rays on

CTM with AHA structure have been investigated in our work. As the results suggest, TID radiation causes the loss of storage electrons. The physical mechanisms are the emission of storage electrons and excess charge generation in the gate oxide. The degradation processes may be aggravated by positive gate bias during the TID radiation. The stored charges may be difficult to lose by deeper trap energy levels and narrower distribution in the trapping layer, while wider bandgap blocking oxide may suppress the radiation-induced charge generation. These methods can be employed to mitigate TID radiation effects of CTM devices for aerospace applications.

References

[1] Guterman D C, Rimawi I H, Chiu T L, Halvorson R D and McElroy D J 1979 *IEEE J. Solid-State Circuits* **14** 498
[2] Kim K and Choi J 2006 *21st IEEE Non-Volatile Semiconductor Memory Workshop* (USA, Monterey 12–16 Feb 2006) p 9
[3] Prall K 2007 *22nd IEEE Non-Volatile Semiconductor Memory Workshop* (USA, Monterey 26—30 Aug 2007) p 5
[4] Lu C Y, Hsieh K Y and Liu R 2009 *Microelectron. Eng.* **86** 283
[5] Houdt J V 2011 *Curr. Appl. Phys.* **11** 21
[6] Molas G, Bocquet M, Vianello E, Perniola L, Grampeix H, Colonna J P and Bongiorno C 2009 *Microelectron. Eng.* **86** 1796
[7] White M H, Adams D A and Bu J 2000 *IEEE Circuits Devices Mag.* **16** 22
[8] Li D M, Wang Z H, Huangfu L Y and Gou Q J 2007 *Chin. Phys.* B **16** 3760
[9] Qiao F Y, Pan L Y, Yu X, Ma Z H, Wu D and Xu J 2014 *Sci. Chin. Inf. Sci.* **57** 1
[10] Tausch J, Tyson S and Fairbanks T 2007 *IEEE Radiat. Eff. Data Workshop* (USA Honolulu 23–27 July 2007) p 189
[11] Bassi S and Pattanaik M 2014 *18th International Symposium on VLSI Design and Test* (India, Coimbatore 16–18 July 2014) p 1
[12] Yao Y, Li C, Huo Z L, Liu M, Zhu C X, Gu C Z, Duan X F, Wang Y G, Gu L and Yu R C 2013 *Nat. Commun.* **4** 2764
[13] Xu Y N, Bi J S, Xu G B, Xi K, Li Bo and Liu M 2017 *Sci. Chin. Inf. Sci.* **60** 120401
[14] Yilmaz E and Kaya S 2016 *IEEE Trans. Nucl. Sci.* **63** 1301
[15] Zhang E X, Fleetwood D M, Hachtel J A, Liang C, Reed R A, Alles M L and Pantelides S T 2016 *IEEE Trans. Nucl. Sci.* **99** 1
[16] Jiang R, Zhang E X, Zhao S E, Fleetwood D M, Schrimpf R D, Reed R A and Doolittle W A 2017 *IEEE Trans. Nucl. Sci.* **99** 1
[17] Choi W H, Park S S, Choi K I, Nam D H, Kwon H M, Han I S and Lee H D 2009 *Jpn. J. Appl. Phys.* **48** 04C068
[18] Felix J A, Schwank J R, Fleetwood D M, Shaneyfelt M R and Gusev E P 2004 *Microelectron. Reliab.* **44** 563
[19] Ergin F B, Turan R, Shishiyanu S T and Yilmaz E 2010 *Nucl. Instrum. Methods Phys. Res. Sect.* B **268** 1482
[20] Lan X X, Ou X, Lei Y, Gong C J, Yin Q N, Xu B, Xia Y D, Yin J and Liu Z G 2013 *Appl. Phys. Lett.* **103** 192905